Investigation of Zeff discrepancy. Complex atom modeling for fusion spectroscopic diagnostics, exploitation of complex spectra for diagnostic purposes

Viorica Stancalie

National Institute for Laser, Plasma and Radiation Physics, Bucharest

The contribution to the JET 2003-2004, TF-D, Workprogramme EFDA (02) –16/4.3 refers to the following Topics endorsed by the EFDA Steering Committee: System Optimization (Topic 10) and Development of ITER heating scenarios and diagnostics (Topic 11) (Order JW3-O-MEC-02.01, Commission No: FU05-CT-2002-00235 & FU05-CT-2003-00205).

On the basis of the selected experiments we contributed on the following tasks:

- Reconciliation between the two methods (visible bremsstrahlung and charge exchange recombination) of measuring Zeff on JET and technique for keeping both diagnostics system *synchronized*
- Complex atom modeling for fusion spectroscopic diagnostics, exploitation of complex spectra for diagnostic purposes, theoretical emission data associated with the diagnostics available (wavelength range and resolution of a particular instrument).

1. Investigation of Zeff discrepancy (S/T Tasks: D-10.1, D-10.3, D-10.4)

The averaged effective ion charge of plasma represents a global quantity characteristic for the confined plasma, which is determined by local values of impurity densities, electron densities and electron temperatures. Each of those quantities is a constant on a magnetic flux surface. Any line of sight integrated measurement of the continuum radiation leading to a line-of-sight averaged value of Zeff is then representative for a specific minimum normalized minor radius associated with the magnetic flux surface tangential to the line of sight. There are currently two main methods for determining Zeff on JET: 1) line integral of the visible, line-free, bremsstrahlung, and 2) charge exchange analysis of dominant impurities. For some time there has been a discrepancy between Zeff as measured by the charge exchange system and the visible continuum spectrum. The aim of this collaboration is to probe possible reasons that may contribute to resolving the discrepancy and use this information to improve the routine data analysis.

We contributed to this milestone analyzing density profiles used in analysis of the KS5 data (toroidal view -radial profile from the charge-exchange diagnostics) which also sees visible bremsstrahlung, VB, and the visible bremsstrahlung measurements from KS3

spectrometer, and on the statistical analysis discrepancy, building a new model and numerical code to calculate bound-free and free-free Gaunt factors accounting for the position of atomic states of large angular momentum. Results can be summarized as follows:

a) Comparative studies with respect to the ratio of horizontal to vertical from visible bremsstrahlung (KS3.Zefh, KS3.Zefv), ratio of horizontal to vertical continuum signal (Edg6.Bash, Edg6.Basv), ratio of Zeff from VB seen by KS5 to that of KS3 (CXSM.ZFBR, KS3.ZEFV and ZEFH). Some examples are shown in the Figure1.

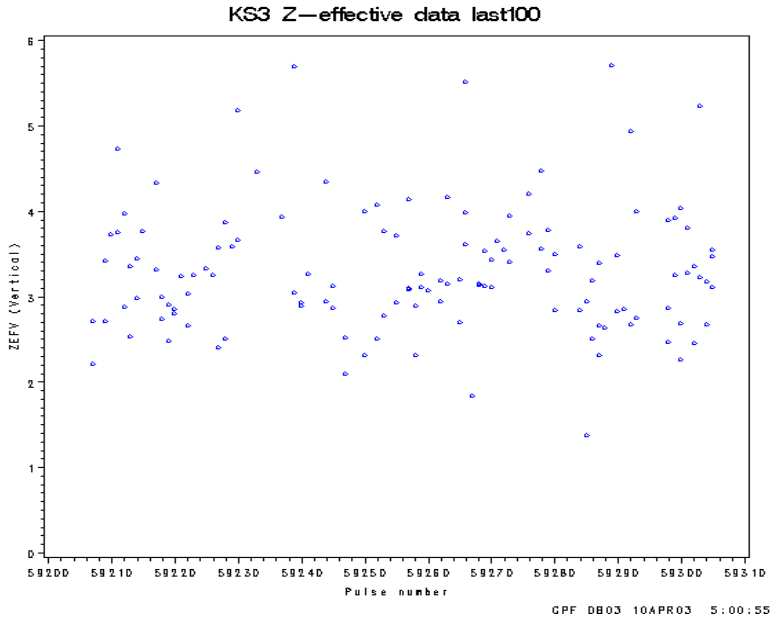

Figure 1. Zeff data from KS3, vertical line of sight, for a sequence of pulses

a) Use KS3 profiles and map n_e and T_e profiles along the line of sight; calculate bremsstrahlung intensities integrating along the line of sight; compare experimental and theoretical intensities. Results were considered for a further analysis of the Gaunt factors. In Table 1 are shown theoretical results for the horizontal line of sight integrated bremsstrahlung intensities.

Table 1. Ks3 –integrated bremsstrahlung intensities along horizontal line of sight

Pulse number	I (horiz) ph/cm^2/sr/s
61005/22.09.2003	4.30808e09
61007	3.86768e11
61010	3.9805e10
61011	3.8637e10
61012	3.88822e10
61013	3.79081e10
61014	3.76684e10
61015	5.045965e10
61017/23.09.2003	6.57251e10
61018	6.39536e10
61019	6.265106e10
61020	6.128258e10
61021	6.72737e10
61022	7.28468e10
61023	9.151816e10
61024	8.59573e10
61025	9.364194e10

b) Location of any free-bound edges and effect of using a mean Gaunt factor or species mix for background bremsstrahlung.

At the moment, there is not a dedicated diagnostic to measure Zeff on JET plasma. It can be derived from VB measurements. The only signals required are the line integrated electron density, n_e , and bremsstrahlung signals, the peak of the electron temperature, T_e, and path length through the plasma. Profile effects are totally ignored. The analysis requires a) renormalize LIDAR n_e to the KG1V.LID3 spectrometer(calibration) data every time; b) map n_e and T_e profile along line-of-sight and c) calculate integral $I(\lambda) = g(\lambda) \int_{LOS} \frac{Z_{eff}\, n_e^2}{\sqrt{T_e}}$. Then $Z_{eff} = I_{measured} / I_{calculated}$. Gaunt factor is calculated for hydrogenic species only, using radial wave functions in the pure Coulomb regime. Figure 2 shows, as an example, the use of the Gaunt factor, total horizontal and vertical path length, TOTH and TOTV, respectively, in *m* units, line-of-sight integrated electron density NEDL, in 10^{20} m^{-2} units, the peak of electron temperature, TMAX, in 10^3eV units, into the calculation of the mean horizontal Zeff (KADH), mean vertical Zeff (KADV) and mean Zeff (KAD), respectively, versus time, for pulse #58870 .

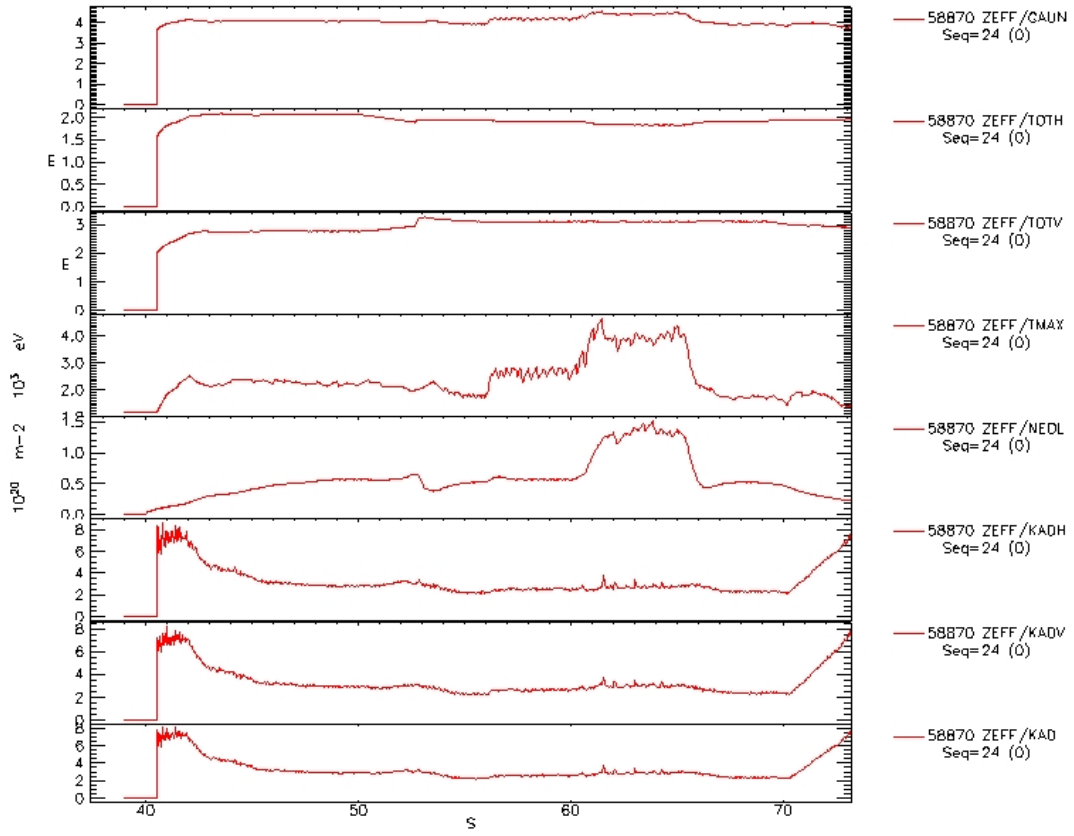

Figure 2. Processed Zeff from visible bremsstrahlung , KS3 data, for pulse # 58870

Based on the previously reported works [1-3] on highly excited Rydberg states in Be-like Al and C ions, we proposed an extension of the use of Rydberg states in the Coulomb formalism accounting for the general properties of the Coulomb Green's function, together with its available compact integral representations and discrete state expansions [4,5].

Coulomb bound-free matrix elements have been computed numerically, avoiding the complex problem of uniform asymptotic expansion. One way to get around this is to introduce the so-called 'averaged excitation energy'. Although, for dipole couplings the integrands can be, in principle, evaluated exactly performing the integration running onto continuous spectrum without severe technical difficulties. These representations are most useful as they provide elegant and efficient ways to compute values of high-order perturbative matrix elements in hydrogen, position of high Rydberg states, autoionization probabilities , oscillator strength averaged over continuous spectrum, and consequently Gaunt factors for non- fully ionized complex atoms. Such calculations are of interest as they represent accurate benchmark data for beam emission spectroscopy, Zeff analysis or complex atoms modeling in fusion plasma devices .

In Figure 3 (*a*,*b*) are presented part of results referring to Gaunt factor for C^{3+}.

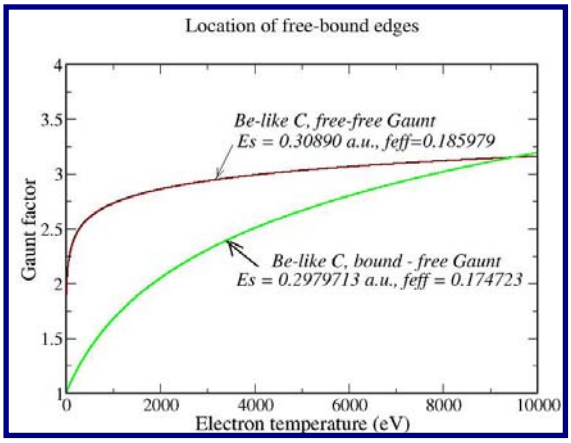

Figure 3a. The Gaunt factors versus the electron temperature (in eV units), for C^2. The 'averaged excitation energy', E_s, in atomic units (a.u) and the effective oscillator strength, f_{eff}, averaged over the continuum, are given next to the curves

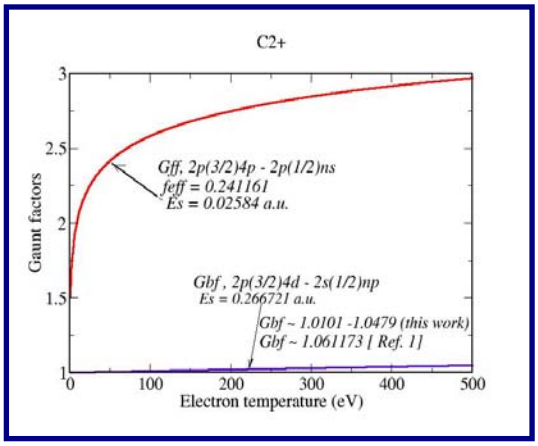

Figure 3b. Free-free Gaunt factor (Gff) and bound free Gaunt factor (Gbf) in C^{2+}, plotted versus electron temperature (eV), for given photon energies (E_s) in atomic units(a.u.). Comparisons with other results [Reference 1] are provided for Gbf.

2. Complex atom modeling for fusion spectroscopic diagnostics, exploitation of complex spectra for diagnostic purposes (S/T Task: D-11.1)

The theoretical issues addressed here are: a) Position of atomic states of large angular momentum; b) Asymptotic expansion of the matrix elements for large angular momentum, together with fixed energy recursion relations between pairs of successive angular momentum states; c) Exchange and fine structure effects in autoionizing doubly excited Rydberg states.

Based on the atomic structure code of Cowan[6] for parent ion states and a new perturbative approach for quasi-continuum states, the model considers a perturbative approach for doubly excited level position, the atomic system being [7,8] described by a closed-shell core and two active electrons, named valence with coordinates referred through index 2, and Rydberg electron the coordinates of which are referred through index 1. For example,

Ba-like W^{18+} has configuration [Xe] $6s^2$, Sr-like W^{36+} has [Kr]$5s^2$ Hf-like W^{2+} has [Xe] $4f^{14}5d^26s^2$,etc. These configurations can be written as [Xe] $n_2l_2j_2n_1l_1$, for Ba-like and in a similar form for the others. The quasi-continuum states are of type $5d_{5/2}nf$ (J=5) or $6p_{3/2}nh$ in Ba-like W^{36+} with decay channel $5d_{5/2}nl \rightarrow 5d_{3/2}\varepsilon'l$ and a such spectra may be grass-like in their complexity. To account theoretically for such transitions, one has to consider the quadrupolar term in the electronic structure. The proper description of a system is the intermediate pair-coupling scheme, *jk*. Then, in a single configuration description, the Rydberg electron is assumed to evolve from a bound hydrogenic state (n_1l_1) to a continuum state (εl) while the valence electron falls from the excited ionic state ($n_2\ l_2\ j_2$) to a lower state ($n_0l_0\ j_0$). The valence electron strongly interacts with the core; hence the spin-orbit effect for this electron dominates all other interactions. The electronic repulsion $1/\ r_{12}$ is generally stronger than spin-orbit effects for the Rydberg electron. Finally, a *jk* or *jl*-coupling scheme is more appropriate for a system. The only thing that changes when different iso-electronic sequences are considered is the Slater integrals and parent ion term. This parent term energy has been calculated by using the atomic structure code of Cowan that allows us to consider *LS* or intermediate coupling scheme. Preliminary results as output from the code: Ba-like W ion, ground configuration [Xe] $6s2(^1S_0)$, are shown in Table 2. Calculated parent ion energy: [Xe]6s = -3480864.083 ($1000cm^{-1}$ units). Table 3 gives results for dipole matrix elements and accuracy as output from the use of Slater or general form for the corresponding radial wavefunction.

Table 2. Atomic data related to selected transitions of interest in Ba-like W ion: E_0, E_1 are energies for the lower and upper configuration, respectively, J_0, J_1 are the corresponding JJ coupled channels, gf and gA are weighted oscillator strengths and radiative transition probability, respectively, and λ is the wavelength corresponding to the considered transition $0 \rightarrow 1$. In the Table values of type 1.5^{09} read $1.5x10^9$.

Config.	J_0	E_0 ($\times 1000$ cm^{-1})	Config.	J_1	$\Delta E=E_1-E_0$ ($\times 1000$ cm^{-1})	λ(Å)	gf	gA (sec^{-1})
$6s^2(^1S_0)$	0.0	-0.0407	$6s7d_{3/.2}(^2S_{0.5})$	2.0	1037.6895	96.3679	0.00002	1.575^{07}
$6s^2(^1S_0)$	0.0	-0.0407	$6s7d_{5/.2}(^2S_{0.5})$	2.0	1047.0111	95.5100	0.00009	6.711^{07}
$6s^2(^1S_0)$	0.0	-0.0407	$6s8d_{3/2}(^2S_{0.5})$	2.0	1369.7852	73.0041	0.00002	1.998^{07}
$6s^2(^1S_0)$	0.0	-0.0407	$6s8d_{5/2}(^2S_{0.5})$	2.0	1375.0632	72.7239	0.00005	6.253^{07}
$6s^2(^1S_0)$	0.0	-0.0407	$6s9d_{3/2}(^2S_{0.5})$	2.0	1579.1392	63.3256	0.00001	1.910^{07}
$6s^2(^1S_0)$	0.0	-0.0407	$6s9d_{5/2}(^2S_{0.5})$	2.0	1582.5176	63.1905	0.00003	5.276^{07}

Table 3. Results for dipole matrix elements of type < 6snl /r/ 6sn'l' > in Ba-like W ion. In the Table, 'frac'represents the ratio between a given Slater integral and the integral of the absolute value of the radial wave function.

nl	*n'l'*	< 6s*nl* |r| 6s*n'l'* > atomic units	frac
7s	7p	2.2898256	-1.600
7s	8p	-0.3172585	0.1927
7s	9p	-0.1535179	0.1335
8s	7p	-0.8260802	0.4506
8s	8p	3.2120362	-0.9990
8s	9p	-0.4231924	0.1784

References:

[1] **Stancalie V.**, *Report presented at the ADAS project meeting*, September 2004, Cadarache, France;

[2] **Stancalie V.**, "*$1s^2 2pns(^1P^0)$ autoionisation levels in Be-like Al and C ions*", Physics of Plasmas 12, 043301(2005);

[3] **Stancalie V.**, "*MQDT/R-matrix Floquet for Dielectronic Recombination", Paper submitted for presentation at the International Conference on Superstrong Fields in Plasmas" Villa Monastero, Varenna(Lc),Italy September 19-24, 2005.*

[4] **Stancalie V.** and **JET-EFDA Contributors**, "*New method to calculate Gaunt factor for the refinement of Zeff evaluation in fusion plasmas*", Paper submitted for presentation at the 32nd EPS Plasma Physics Conference, Tarragona, Spain, 27 June – 1 July 2005;

[5] **Chelmus A. R. D.**, **Stancalie V.**, "*Radiative Gaunt factor*" Proc. of the Seventeenth European Conference on Atomic and Molecular Physics of Ionized Gases, 1-5 September 2004, Constantza, Romania, 76-77, to be published in Journal of Advanced Materials and Optoelectronics, Vol.4 (2005).

[6] Cowan, R. D., "*The Theory of Atomic Structure And Spectra*", University of California Press, Berkley, California, 1981.

[7] **Stancalie V.**, **Mihailescu A.**, "*Complex Atoms Modeling for Plasma Diagnostics*" Proc. of the Seventeenth European Conference on Atomic and Molecular Physics of Ionized Gases, 1-5 September 2004, Constantza, Romania, 82 –83, to be published in Journal of Advanced Materials and Optoelectronics, Vol.4 (2005).

[8] **Mihailescu A.**, **Stancalie V.**, **Pais V.**, **Chelmus A. R. D.**, "*Atomic data for Zn-like W ions as related to the plasma modeling*" Paper submitted for presentation at the 32nd EPS Plasma Physics Conference, 2005, Tarragona, Spain, 27June-1July,2005.